ARTICLES

Comparison between Experimental and Three-Dimensional Quantum Mechanical Rate Constants for the NH(D) + NO Reactions

Henrik Szichman and Michael Baer*

Department of Physics and Applied Mathematics, Soreq NRC, Yavne 81800, Israel

H. R. Volpp and J. Wolfrum

Physikalisch-Chemisches Institut der Universitat Heidelberg, Im Neuerheimer Feld 253, 69120 Heidelberg, Germany

Received: July 2, 1998

We describe a three-dimensional quantum mechanical study within the nonreactive infinite order sudden approximation (IOSA) for the title systems. The study was performed using a recently introduced global potential energy surface (Bradley et al. *J. Chem. Phys.* **1995**, *102*, 6696). Integral total cross sections for the two reactions, namely, NO + NH and NO + ND, were calculated as a function of kinetic energy in the range 0.05−0.50 eV. Using these cross sections, temperature-dependent rate constants were calculated. Our main findings are: (a) The energy-dependent cross sections for the two isotopic reactions are very similar; still, the cross sections for NO + NH are larger at the low-energy region while those for NO + ND are somewhat larger at the high-energy region. (b) The two cross section curves start to increase at zero kinetic energy, indicating the absence of a potential energy barrier or the existence of a mild one at most. (c) Compared with quasi-classical-trajectory cross sections the present quantum mechanical cross sections for NH + NO are half as large at the low energy region but tend to become similar at the higher one. (d) The calculated rate constants for NH + NO were compared with experiment (for a wide range of temperatures) and with one quasi-classical trajectory result (at $T = 300$ K). There is a very encouraging agreement at the high-temperature region ($1200 \leq T \leq 5000$ K) but large discrepancies (1 order of magnitude difference) at low temperatures. The fit with the (single) classical result was reasonably good. (e) Rate constants calculated for ND + NO were found to be very similar to the rate constants of NH + NO. A single measured value, $k(T = 300\ \text{K}) = (2.7 \pm 0.4)\ 10^{-11}$ molec^{-1} cm^3 s^{-1}, reported here for the first time, is equal to half the corresponding value for NH + NO, namely, $k(T = 300\ \text{K}) = (5.5 \pm 0.3) \times 10^{-11}$ molec^{-1} cm^3 s^{-1}, and it therefore fit the QM curve slightly better.

I. Introduction

Nitrogen oxides (NO_x) from combustion processes which use fossil fuels (such as in burners, furnaces, incinerators, motor cars, etc.) are among the most harmful environmental pollutants.[1] Of these, the pollutant emitted in largest quantity is NO, which, although not so deleterious *per se*, is potentially noxious in that it forms NO_2 (by reacting with O_2), which is hazardous to human health.[1] Consequently, extensive efforts are being invested to find ways to remove NO or to at least reduce its rate of emission into the atmosphere. One way to achieve this goal has received a lot of attention in recent years and that is to let NO react with NH_x; $x = 1, 2$ radicals.[2] In this article we concentrate on the reactions of NO with NH and ND and calculate energy-dependent cross sections and rate constants for the two isotopic reactions:

$$\text{NH} + \text{NO} \rightarrow \{\text{N}_2\text{O} + \text{H};\ \text{N}_2 + \text{OH}\} \quad \text{(I)}$$

$$\text{ND} + \text{NO} \rightarrow \{\text{N}_2\text{O} + \text{D};\ \text{N2} + \text{OD}\} \quad \text{(II)}$$

To date, experimental studies of reaction I have focused on measurements of rate constants. In general these fell into two categories: (a) studies measuring the overall rate constants[3−5] and (b) studies measuring the branching ratio of the two possible products.[3d−h,4,5] The majority of the overall rate constant measurements were done at room temperature and there is a good agreement between the various results (estimated to be in the range $(3.8 - 5.8) \times 10^{-11}$ molec^{-1}cm^3 s^{-1}). A number of rate constants were measured as a function of temperature; Harrison et al.[3d] found the rate constants to be at most weakly dependent on the temperature (but the measurements were done only along a short temperature range, i.e., $269 \leq T \leq 377$ K), and Lillich et al.[4] who performed their studies along a larger temperature range, namely, $300 \leq T \leq 1000$ K, found a slight negative dependence. There is much less agreement regarding

* Corresponding author.

10.1021/jp9828641 CCC: $15.00
Published on Web 12/02/1998

the branching ratios, although the numbers are slowly converging (at $T = 300$ K) to a definite value. However, since this subject will not be considered here we shall not elaborate on it.

Reaction I and the relevant branching ratio were studied numerically.[6−8] Part of these studies are transition-state-type treatments[6] based on features of the potential energy surface (PES) along the reaction coordinate, as calculated by Durant[5] and by Walch.[9] Transition-state-theory has been successfully applied on many occasions[10] but it is not always obvious whether it really has a predictive power or is only a kind of a fitting process. Two 3-dimensional (3D) dynamical treatments were recently published, namely the quasi-classical-trajectory (QCT) study performed by Bradley et al.,[7] and a quantum mechanical (QM) study performed by Szichman and Baer.[8] Both were carried out on an improved version of Walch's PES.[9] In the QCT treatment the overall rate constants were found to be weakly dependent on the temperature and about 5 times smaller than the experimental values. As for the QM results it was found that the cross sections were about 1−3 times smaller (depending on the energy) than the QCT results, and therefore the discrepancy with regard to the experimental rate constants was larger. In the present publication we shall report on somewhat modified results obtained by following a more careful tuning of the numerical parameters that control the calculations.

As for the isotopic reaction (II), it has so far not been studied, either experimentally or theoretically. In the present article, we report on the first experimental and theoretical rate constants (and QM cross sections) for this reaction.

In the theoretical part of this article we present a three-dimensional QM study, carried out within the infinite order sudden approximation (IOSA). Tetra-atom reactive systems have recently become a rather popular subject in the field of QM reactive scattering.[11−15] The introduction of the negative imaginary potentials (NIP)[16] to decouple arrangement channels (AC)[17] is responsible for most of the achievements in this area, among which are an exact 6D ($J = 0$) calculation for the $H_2 + OH$ reaction,[11g] a 6MD coupled-states calculation of cross sections for the $H_2O + H$ reaction,[14] and several 5MD coupled-states calculations that yielded state-selected cross sections and rate constants.[11e,f,15] In our group we considered a number of reactive systems, most of them within the IOSA (or extended versions of it), which are 3D calculations with the three Jacobi angles treated as parameters selected randomly by a Monte-Carlo procedure. Despite its relative simplicity this approximation yielded, for tri-atom[17a] and tetra-atom reactions treated as single AC systems, results which are close to those obtained with less approximate methods.[13] We applied this method to $O + O_3 \rightarrow 2O_2$,[12] for which the calculated rate constants fit the experiments very nicely, and to $H_2 + OH \rightarrow H_2O + H$ reaction,[13] for which the cross sections were in a reasonable agreement with 6MD[15] and several 5MD coupled-states calculations.

II. Theory

The method[17] is based on the idea that the numerical treatment can be carried out in the reagents' AC only, and the fact that reactions occur is treated by substituting NIPs[16] at the entrances to each of the exchange (reactive) ACs. This procedure, which decouples the exchange ACs, avoids the need to treat the Schroedinger equation in the different products ACs and consequently eliminates the complicated transformations between the various sets of Jacobi coordinates.

II.1. The Perturbed-like Schroedinger Equation. Our theoretical treatment is based on deriving a (non-reactive) **S** matrix element, which is given in the form

$$\mathbf{S}(t \leftarrow t_0) = (\delta_{tt_0} + i\langle\psi_t|V|\Psi_{t_0}\rangle)\exp(i\varphi_t) \quad (1)$$

where ψ_t (and ψ_{t_0}) is a solution of an unperturbed (elastic) Schroedinger equation (SE), namely

$$(E - H_0)\psi_t = 0 \quad (2)$$

Ψ_{t_0} is a solution of the full SE, namely

$$(E - H)\Psi_{t_0} = 0 \quad (3)$$

V is the perturbation potential defined as $H - H_0$, φ_t is the tth (elastic) phase shift, and t and t_0, respectively, designate a set of quantum numbers related to the AC under consideration. The reactive transition probability is obtained from the expression

$$P_{\text{react}} = 1 - \sum_t |\mathbf{S}(t \leftarrow t_0)|^2 \quad (4)$$

To derive the **S** matrix elements we must first calculate Ψ_{t_0}, and this we do by employing the perturbative-type approach, namely, presenting Ψ_{t_0} as a sum of two functions:

$$\Psi_{t_0} = \chi_{t_0} + \psi_{t_0} \quad (5)$$

where ψ_{t_0} is the solution of eq 2 and χ_{t_0} can be shown to be the solution of the inhomogeneous equation:

$$(E - H)\chi_{t_0} = V\psi_{t_0} \quad (6)$$

Equation 6 describes all processes, reactive and nonreactive. To make it adequate for studying nonreactive processes only, appropriate NIPs must be added to H, in order to impose outgoing boundary conditions. As a result, a new Hamiltonian, H_I, is formed (for more details see refs 16a and 17) and consequently eq 6 becomes

$$(E - H_I)\chi_{t_0} = V\psi_{t_0} \quad (7)$$

Equation 7 is the equation solved in the numerical study.

II.2. The Infinite-Order-Sudden-Approximation (IOSA) for the Diatom−Diatom Hamiltonian. The 3D IOSA hamiltonian for the diatom−diatom system takes the form[11i]

$$H = -\frac{\hbar^2}{2\mu_1 r_1^2}\frac{\partial^2}{\partial r_1^2}r_1 - \frac{\hbar^2}{2\mu_2 r_2^2}\frac{\partial^2}{\partial r_2^2}r_2 - \frac{\hbar^2}{2\mu R^2}\frac{\partial^2}{\partial R^2}R + \hbar^2\frac{j_1(j_1+1)}{2\mu_1 r_1^2} + \hbar^2\frac{j_2(j_2+1)}{2\mu_2 r_2^2} + \hbar^2\frac{J(J+1)}{2mR^2} + U(r_1 r_2 R|\gamma_1\gamma_2) \quad (8)$$

where r_i, μ_i, and j_i ($i = 1, 2$) are the interatomic distances, the reduced masses, and the rotational quantum numbers, respectively, related to the two diatomics, J is the total angular momentum quantum number, R is the translational distance, μ is the corresponding reduced mass of the whole system, and γ_i is the angle between $\hat{r}_i$ and $\hat{R}$. It is well noticed that ϕ, the angle formed by the two ($\hat{r}_i$, $\hat{R}$) ($i = 1, 2$) planes, is missing. In some of our previous treatments it was explicitly included in the Monte−Carlo selection of the frozen IOSA angles, but recently we found out that eliminating the angle ϕ by employing a *ϕ-averaged* PES yields reliable results.[13] Equation 7 is solved with the Hamiltonian H given in eq 8 and with γ_1 and γ_2 being

parameters changed from one calculation to another. Equation 2 is solved with a similar Hamiltonian except that a different potential is used, namely, $U(r_1r_2R|\gamma_1\gamma_2)$ is replaced by

$$U_0(r_1r_2R|\gamma_1\gamma_2) = v_1(r_1) + v_2(r_2) + w(R|\gamma_1\gamma_2) \qquad (9)$$

where $v_i(r_i)$ ($i = 1, 2$) are the diatomic potentials and $w(R|\gamma_1\gamma_2)$, the distortion potential, is defined as

$$w(R|\gamma_1\gamma_2) = U(r_{1e}r_{2e}R|\gamma_1\gamma_2) \qquad (10)$$

Here r_{ie} is the ith diatomic internal equilibrium distance.

III. Numerical Details

The present study was carried out on a PES originally calculated by Walch[9] and recently extended by Bradley et al.[7] In fact, the latter group suggested two different PESs; we employed the one labeled "Surface I".

To perform the calculations, the reagents translational range (1.3−5.2 Å) was divided into 120 equidistant sectors; at each sector the χ-wave function was presented in terms of a Gaussian, which stands for the translational part, and a set of adiabatic (r_1r_2) dependent basis functions. The size of the basis set at each sector is controlled by a given energy value (for details see ref 11i). Altogether the χ-wave function was expressed in terms of about 3000 basis sets.

Three Neuhauser−Baer linear-ramp NIPs were used in the calculations: one along the translational coordinate R with the parameters (ΔR_I, u_I) ≡ (1 Å ,0.2 eV) and one along each of the vibrational coordinates r_i ($i = 1, 2$) with the parameters (Δr_{iI}, u_{iI}) ≡ (0.8 Å ,0.3 eV) ($i = 1, 2$). Here ΔR_I and Δr_{iI} are the R and the r_i intervals along which the NIP differs from zero, and u_I and u_{iI} are the corresponding heights of the NIPs. As mentioned before, the R range along which the full wave function was calculated as 1.3−5.2 Å and the corresponding ranges of r_1(NH) and r_2(NO) are 0.7−2.5 Å and 0.8−2.45 Å, respectively.

A separate calculation was performed for each J. The range of J for the highest energy was (0, 200) and the grid size was $\Delta J = 20$. As mentioned earlier, the size of the basis set was 3000 (3500 for the isotopic case); this means that for each J, for each set of ($\gamma_1\gamma_2$) angles and for each energy we had to solve 3000 (3500) complex algebraic equations. It is of interest to mention that a similar calculation for H_2 + OH was done with 600 equations only.

In the previous numerical treatment[8] the two frozen γ_i; ($i = 1, 2$) angles were selected randomly, employing the Monte Carlo method. The present calculation is carried out using a fixed rectangular grid for z_i (=cos(γ_i)); ($i = 1, 2$). We established that with this procedure we attained a higher accuracy. To this end the range of z_1(NH) was chosen as (−1.0, 1.0) but the range for z_2(NO) was found to be much shorter, namely, (0.625, 1.0). The corresponding grid sizes were (Δz_1, Δz_2) = (0.25, 0.125). Thus calculations were done for 36 different sets of (γ_1, γ_2) values.

IV. Results and Discussion

IV.1. Reactive Cross Sections. The emphasis in the present study is on reactions from the ground state only. Figure 1 shows our total integral reactive QM cross sections for reaction I, and the following are to be noted:

(a) The cross section curve, $\sigma(E_{tr})$, starts to increase right from $E_{tr} = 0.0$, indicating the absence of a potential barrier or the existence of a very low one, at most. This increase continues up to $E_{tr} = 0.1$ eV, where the cross section curve reaches the value of $\sigma \sim 10$ bohr^2. From there on $\sigma(E_{tr})$ remains constant.

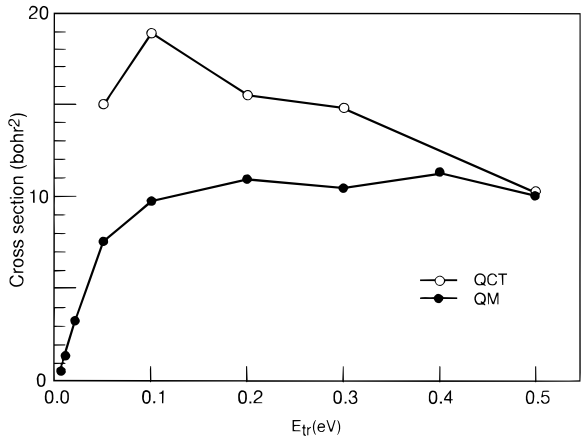

Figure 1. Comparison between QM and QCT cross sections for NH + NO → (products): (●) quantum mechanical results (present); (○) quasi-classical trajectory results (ref 7).

(b) For comparison we also present QCT cross sections. Since numerical values were published only for $E_{tr} \geq 0.05$ eV, the QCT cross sections behavior at threshold is not known, although it is most likely that the threshold is also at $E_{tr} = 0.0$ and not at a higher energy. However, the QCT $\sigma(E_{tr})$ behaves altogether differently. It increases, eventually, with the same rate but reaches a higher value, i.e., $\sigma \sim 18$ bohr^2, which is about 2 times larger than in the QM treatment. From there on the curve starts to decrease along the whole reported energy interval 0.1 $\leq E_{tr} \leq$ 0.5 eV.

(c)The QM cross sections are 1−2 times smaller than the QCT ones; the largest differences are at the lower energy end, but as the energy increases the two types of results approach each other, so that at $E_{tr} \sim 0.5$ eV the two become very close. The reason the two types of results differ considerably at the lower energy end could be the fact that the QM cross sections are only approximate. However, in our opinion it is more likely a quantum effect associated with the inability of classical mechanics to conserve the zero point energy (ZPE) along the reaction coordinate. This problem was discussed for the H_2 + CN system[18a] and more recently also for the H_2O + H system.[18b,c] (For QM calculations for the H_2O + H system, see refs. 13 and 15.) It is important to mention that the fit between the QCT and the QM cross sections, in both cases, improved significantly once the trajectories, which led to products with internal energies below the ZPE were eliminated.

Before closing this subject we shall comment on our previous publication on this subject,[8] which reported cross sections smaller by about 20−30%. The difference is mainly attributable to the fact that one of the NIP parameters, the translational potential height u_{IR}, was not well tuned.

In Figure 2 are presented the energy-dependent cross sections $\sigma(E_{tr})$ for reaction II. We also show, for comparison, the cross sections for reaction I. It is well noticed that in the low-energy region the cross sections for reaction I are significantly higher than those for reaction II, but once $E_{tr} \rightarrow 0.05$ eV the cross sections for reaction II become somewhat larger (by less than 10%). Still, the deviations are not significant enough (due to the IOSA) to permit drawing any conclusions regarding a difference in the mechanisms of the two reactions.

IV.2. Rate Constants. Figure 3 shows the calculated rate constants for reaction I compared with experimental results reported by various groups.[3g,i,j,4] Also presented is a single QCT result at $T = 3000$ K.[7] It is noticed that, at the high-temperature

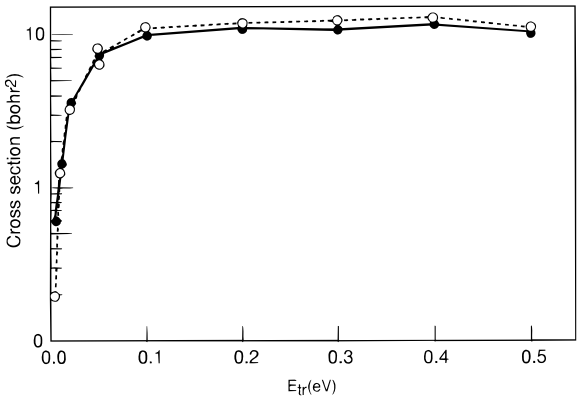

Figure 2. Comparison between the QM cross sections of the reaction NH + NO and the reaction ND + NO: (●) QM cross sections for NH + NO → (products); (○) QM cross sections for ND + NO → (products).

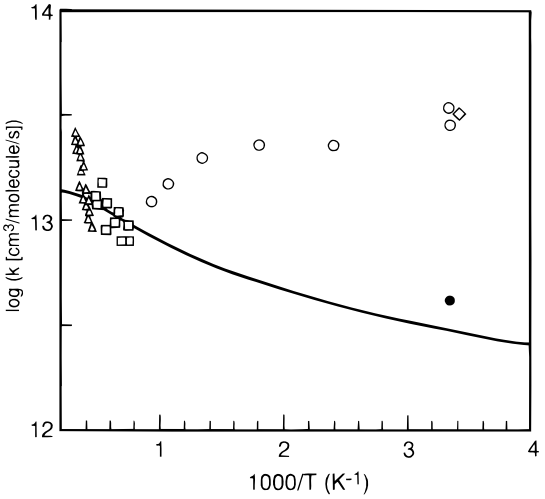

Figure 3. Comparison between QM, experimental, and QCT rate constants for NH + NO → (products): (—) present QM rate constant; (●) QCT rate constant (ref 7); (◇) experimental results (ref 4); (○) experimental results (ref. 3i); (□) experimental results (ref 3j); (△) experimental results (ref 3g).

region, the experimental rate constants are distributed very nicely around the QM curve. However, as the temperature decreases, the deviations become larger and larger so that at the low-temperature region the two kinds of rate constants grow apart by more than 1 order of magnitude. Moreover, the trend is different: whereas the QM curve decreases uniformly with the temperature, the experimental curve differs in structure: starting at the high-temperature end the rate constant curve decreases relatively fast at first but then, around $T = 1200$ K, it starts to increase, rising by almost 1 order of magnitude. We do not have an explanation for the large discrepancy at the low-temperature interval other than to relate it to the PES used in the numerical treatment. Possibly it results either from inaccuracies in PES itself or eventually the neglect of excited accessible adiabatic electronic states which might enhance the reaction process if the proper nonadiabatic coupling terms were added to the Hamiltonian. In any case, in our opinion this is not due to the frozen γ-angles assumption (namely with the IOSA). This is because our QM rate constant at $T = 300$ K differs by only 20% from the QCT result; QCT calculations were done without freezing any angle. That these two types of calculations yielded similar results does not necessarily mean that the theoretical results are correct but indicates that more work is needed on the PES.

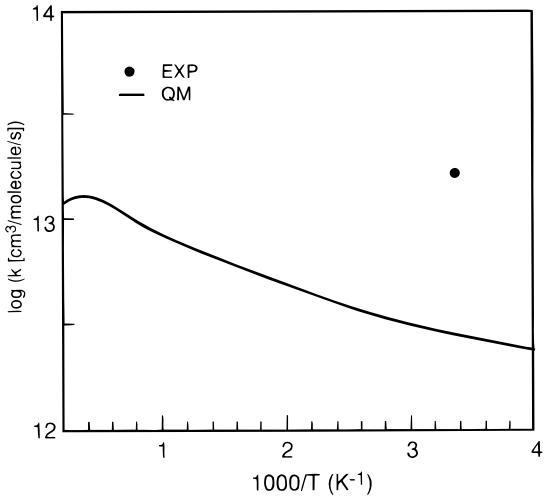

Figure 4. Comparison between QM and experimental rate constants for ND + NO → (products): (—) present QM rate constant; (●) present experimental results.

Figure 4 presents the QM rate constants for reaction II. Unfortunately no experimental rate constants are available except for our own single value (reported in this publication for the first time), which is also presented in the figure. The experimental value was obtained using a pulsed laser photolysis/laser-induced fluorescence (LIF) pump-and-probe technique similar to the one used in our previous study of reaction I.[4] In the present kinetics studies of reactions I and II NH/ND reagents were generated via the well-characterized laser photolysis of HNCO/DNCO at a wavelength of 193 nm.[19] Formation of H/D atoms produced in the reactions of NH/ND with NO was monitored using time-resolved LIF at the H/D atom Lyman α transition.[20] In combination with photolytic calibration method it was possible to determine rate constants $k_I(T = 300\ \text{K}) = (5.5 \pm 0.3) \times 10^{-11}$ molec^{-1} cm^3 s^{-1}) and $k_{II}(T = 300\ \text{K}) = (2.7 \pm 0.4) \times 10^{-11}$ molec^{-1} cm^3 s^{-1}) as well as branching ratios for the H and D atoms product channel: $f_H = (0.78 \pm 0.09)$ and $f_D = (0.76 \pm 0.17)$, respectively. The rate constant and the atom branching ratio obtained for reaction I are in good agreement with previous results.[3i,4,5] For reaction II, as is noticed again, a large discrepancy is observed between the experimental rate constant and the theoretical results, although the deviation is smaller than in case of reaction I.

V. Summary

We have described a three-dimensional quantum mechanical study of the title system in which we used a recently introduced global PES. The numerical treatment was carried out within the nonreactive IOSA where in each calculation the angles ($\gamma_1\gamma_2$) were held fixed (namely served as parameters) and the third, the out-of-plane angle ϕ, was eliminated by using a ϕ-averaged potential. The SE was solved in the reagents AC only, and the exchange ACs were eliminated by using NIPs. Integral total cross sections for the two isotopic reactions (I and II) were calculated, as a function of kinetic energy, in the range 0.05−0.50 eV. These calculations were followed by the derivation of the corresponding rate constants. Our main findings are: (a) The cross sections start increasing right from the beginning at $E_{tr} = 0.0$ eV, reaching their highest value at $E_{tr} = 0.1$ eV, and then staying more or less constant until the end of the considered energy interval, i.e., $E_{tr} = 0.5$ eV. (b) The QM cross sections are about 1−2 times smaller than the corresponding QCT ones. They are seen to become identical at the vicinity of $E_{tr} = 0.5$

eV and probably at threshold. (c) The QM rate constants for reaction I seem to fit quite well the experimental ones at the high-temperature region $1200 \leq T \leq 5000$ K, but significant deviations are observed as the temperature decreases. At $T =$ 300 K the two types of results differ by 1 order of magnitude. A slightly better fit is obtained for reaction II. (d) A good fit is obtained between the QM and the QCT rate constant, at $T =$ 300 K (the only QCT published value). (e) The fact that the theoretical results deviate so significantly from the experimental ones implies that more theoretical studies are needed — some of them related to the PES.

We also report here, for the first time, the experimental rate constant $k(T = 300\ \text{K})$ for the ND + NO reaction, which is $(2.7 \pm 0.4) \times 10^{-11}$ molec^{-1} cm^3 s^{-1}. This value is about 2 times smaller than the corresponding value, namely, $(5.5 \pm 0.3) \times 10^{-11}$ molec^{-1} cm^3 s^{-1}, for reaction I.

Acknowledgment. This research is supported by a grant from the Bundesministerium fur Bildung und Forschung (BMBF, Germany) via Grant No. 1447 and by the Deutsche Forschungsgemeinschaft *via* SFB 359.

References and Notes

(1) Stuck, J. M.; Stephens, E. R. *Adv. Environm. Sci.* **1969**, *1*, 73.

(2) Lyon, R. K.; Benn, D. J. *17th Symp. (Internat.) on Combustion, Comb. Inst.* **1979**. Miller, J. A.; Branchand, M. C.; Kee, R. J. *Comb. Fl.* **1981**, *43*, 81. Dasch, C. J.; Blint, R. J. *GMR-4232*, General Motors Res Lab: Warren, MI, 1982. Miller, J. A.; Bowman, C. T. *Prog. Energy Combust. Sci.* 1989, *15*, 287; Miller, J.A.; Bowman, C. T. *Int. J. Chem. Kinet.* **1991**, *23*, 289.

(3) (a) Gordon, S.; Mulac, W.; Nangia, P. *J. Phys. Chem.* **1971**, *75*, 2087. (b) Hansen, I.; Hoeinghaus, K.; Zetsch, C.; Stuhl, F. *Chem. Phys. Lett.* **1976**, *42*, 370. (c) Cox, J. W.; Nelson, H. H.; McDonalds, J. R. *Chem. Phys.* **1985**, *96*, 175. (d) Harrison, J. A.; Whyte, A. R.; Phillips, L. F. *Chem. Phys. Lett.* **1986**, *129*, 346. (e) Hack, W.; Wagner, H. Gg.; Zasypkin, A. *Ber. Bunsen-Ges. Phys. Chem.* **1994**, *98*, 156. (f) Yamasaki, K.; Okada, S.; Koshi, M.; Matsui, H. *Chem. Phys.* **1991**, *95*, 5087. (g) Mertens, J. D.; Chang, A. Y.; Hanson, R. K.; Bowman, C. T. *Int. J. Chem. Kinet.* **1991**, *23*, 173. (h) Yokoyama, K.; Sakane, Y.; Fueno, T. *Bull. Chem. Soc. Jpn.* **1991**, *64*, 1738. (i) Vandooren, J.; Sarkisov, O. M.; Balakhnin, V. P.; Van Tiggelen, P. J. *Chem. Phys. Lett.* **1991**, *184*, 294. (j) Roemming, H.-J.; Wagner, H.Gg. *26th Symp. (Internat) on Comb., Comb. Inst.* **1996**, 559.

(4) Lillich, H.; Schuck, A.; Volpp, H. R.; Wolfrum, J.; Naik, P. D. *25th Symp. (Internat) on Comb., Comb. Inst.* **1994**, 993.

(5) Durant, J. D. *J. Phys. Chem.* **1994**, *98*, 518.

(6) Melius, C. F.; Binkley, J. S. *20th Symp. (Internat) on Comb., Comb. Inst.* **1984**, 575. (b) Fueno, T.; Fukada, M.; Yokoyama, K. *Chem. Phys.* **1988**, *124*, 265. (c) Harrison, J. A.; Maclagan, R. G. A. R. *J. Chem. Soc. Faraday Trans.* **1990**, *86*, 3519. (d) Melius, C. F.; Binkley, J. S. *24th Symp. (Internat) on Comb., Comb. Inst.* **1993**, p 719.

(7) Bradley, K. S.; McCabe, P.; Schatz, G. C.; Walch, S. P. *J. Chem. Phys.* **1995**, *102*, 6696.

(8) Szichman, H.; Baer, M. *J. Chem. Phys.* **1996**, *105*, 10380.

(9) Walch, S. P. *J. Chem. Phys.* **1993**, *98*, 1170.

(10) Truhlar, D. G.; Isaacson, A. D.; Garret. B. C. In *Theory of Chemical Reaction Dynamics*; Baer; M., Ed.; CRC Press, Inc.: Boca Raton, FL, 1985; Vol. IV; Chapter 2.

(11) (a) Baer, M.; Ng, C. Y. *J. Chem. Phys.* **1990**, *93*, 7787. (b) Clary, D. C. *J. Chem. Phys.* **1991**, *95*, 7248; **1992**, *96*, 3656. (c) Bowman, J. M.; Wang, D. *J. Chem. Phys.* **1991**, *96*, 7852. Bowman, J. M., Wang, D. *J. Chem. Phys.* **1993**, *98*, 6235. (d) Billing, G. D. *Chem. Phys.* **1990**, *146*, 63; **1992**, *161*, 245. (e) Zhang, D. H.; Zhang, J. H. *J. Chem. Phys.* **1993**, *99*, 5615; **1994**, *100*, 2697; **1994**, 101, 1146; **1995**, *103*, 6512. (f) Manthe, U.; Seideman, T.; Miller, W. H. *J. Chem. Phys.* **1993**, *99*, 10078; **1994**, *101*, 4759. (g) Neuhauser, D. *J. Chem. Phys.* **1994**, *100*, 9272. (h) Szichman, H.; Last, I.; Baram, A.; Baer, M. *J. Phys. Chem.* **1993**, *97*, 6436. (i) Szichman, H.; Baer, M. *J. Chem. Phys.* **1994**, *101*, 2081. (j) Echave, J.; Clary, D. C. *J. Chem. Phys.* **1994**, *100*, 402. (k) Balakrishnan, N.; Billing, G. D. *J. Chem. Phys.* **1996**, *104*, 4005.

(12) Szichman, H.; Varandas, A. J. C.; Baer, M. *J. Chem. Phys.* **1995**, *102*, 3474.

(13) Szichman, H.; Baer, M. *Chem. Phys. Lett.* **1995**, *242*, 285. Baer, M.; Szichman, H.; Rosenman, E.; Hochman-Kowal, S.; Persky, A. In *Gas Phase Chemical Reaction Systems*; Wolfrum, J., Volpp, H.-R., Rannacher, R., Warmatz, J., Eds.; Springer Verlag: Berlin, Heidelberg, 1996; p 125.

(14) Zhang, D. H.; Light, J. C. *J. Chem. Phys.* **1996**, *104*, 5615.

(15) Zhang, D. H.; Zhang, J. H. *J. Chem. Phys.* **1994**, *100*, 2697.

(16) (a) Neuhauser, D.; Baer, M. *J. Chem. Phys.* **1989**, *90*, 4351. (b) Kosloff, R.; Kosloff, D. *J. Comp. Phys.* **1986**, *52*, 35. Child, M. S. *Mol. Phys.* **1991**, *72*, 89.

(17) (a) Baer, M.; Ng, C. Y.; Neuhauser, D. *Chem. Phys. Lett.* **1990**, *169*, 534. (b) Baer, M.; Nakamura, H. *J. Chem. Phys.* **1992**, *96*, 6565. (c) Baram, A.; Last, I.; Baer, M. *Chem. Phys. Lett.* **1993**, *212*, 649.

(18) (a) Wagner, A. F.; Schatz, G. C.; ter Horst, M. A. *J. Chem. Phys.* **1997**, *106*, 6001. (b) Bradley, K. S.; Schatz, G. C. *J. Chem. Phys.* **1998**, *108*, 7994. (c) Schatz, G. C. Private Communication.

(19) Brownsword, R. A.; Hillenkamp, M.; Laurent, T.; Vatsa, R. K.; Volpp, H.-R.; *J. Chem. Phys.* **1997**, *106*, 4436.

(20) Brownsword, R. A.; Hillenkamp, M.; Laurent, T.; Volpp, H.-R.; Wolfrum, J.; Vatsa, R. K.; Yoo, H.-S. *J. Phys. Chem.* **1997**, *101*, 6448.